

## Research Article

# An Experimental Study on the Creep Characteristics of Sandstone in the Interval of Different Critical Stresses

Chao Yang , Xingchen Dong, Xuan Xu, and Qiancheng Sun 

Key Laboratory of Geological Hazards on Three Gorges Reservoir Area (China Three Gorges University), Ministry of Education, Yichang 443002, China

Correspondence should be addressed to Qiancheng Sun; qc\_sun@ctgu.edu.cn

Received 18 May 2021; Accepted 24 June 2021; Published 16 July 2021

Academic Editor: Zhigang Tao

Copyright © 2021 Chao Yang et al. This is an open access article distributed under the Creative Commons Attribution License, which permits unrestricted use, distribution, and reproduction in any medium, provided the original work is properly cited.

Creep tests on brittle sandstone specimens were performed to investigate the time-dependent characteristics in the interval of different critical stresses. The results showed that failure will not occur when the loaded stress  $\sigma_1$  is less than the critical stress of dilation  $\sigma_{cd}$ , while all specimens were destroyed when  $\sigma_1$  is larger than  $\sigma_{cd}$ . In addition, the value of  $\sigma_{cd}$  was very close to the long-term strength obtained by the method of the isochronous stress-strain curve. Therefore,  $\sigma_{cd}$  can be regarded as the long-term strength of the sandstone specimens. When  $\sigma_1$  is larger than  $\sigma_{cd}$ , the time required for the failure of specimen  $t_f$  decreases with the increase of  $\sigma_1$ ; the creep rate  $d\varepsilon/dt$  increases with time  $t$ , and the specimen will be destroyed when it reaches a maximum value  $(d\varepsilon/dt)_{\max}$ . Both relationships  $t_f$  and  $\sigma_1$  and  $(d\varepsilon/dt)_{\max}$  and  $\sigma_1$  can be described by the exponential function. Then, a nonlinear damage creep model considering the deformation damage and strength damage in the interval of different critical stresses was established, which can describe the whole creep process and predict the failure time of sandstone specimens.

## 1. Introduction

Critical stresses (the crack closure stress level  $\sigma_{cc}$ , crack initiation stress level  $\sigma_{ci}$ , critical stress of dilation  $\sigma_{cd}$ , and peak strength  $\sigma_c$ ) are important indexes for evaluating hard brittle rocks [1–3], which reflect the internal microfracture activity state of rocks under different stress levels. The failure process of rocks under different compression conditions can be divided into 4 stages, which are crack closure stage ( $\sigma_1 < \sigma_{cc}$ ), elastic region ( $\sigma_{cc} < \sigma_1 < \sigma_{ci}$ ), stable crack growth stage ( $\sigma_{ci} < \sigma_1 < \sigma_{cd}$ ), and unstable crack growth stage ( $\sigma_{cd} < \sigma_1 < \sigma_c$ ). Obviously, the creep characteristics of hard brittle rocks should also be different when under long-term loading in different critical stress intervals.

As the critical point of time-dependent damage under the creep condition, the long-term strength of rocks has always been the focus of researchers [4–6]. Currently, there are mainly two methods to determine the long-term strength. (1) The steady-state creep rate [7]: carrying out creep tests at multiple stress levels by the “Chen method” and determining long-term strength as the maximum load

with zero creep rate. (2) The stress-strain isochronal curves [8, 9]: treating the long-term strength as the yield strength and considering the time effect. Both methods mentioned above are based on a large number of creep tests, which makes the acquisition of long-term strength of rocks relatively complicated. If the results of uniaxial or triaxial tests can be used to establish the correlation with the long-term strength of rocks, the difficulty of the test will be greatly reduced. Some attempts have been made, such as Liu [10] who used the volume expansion method which determines the long-term strength by the volume expansion point and Ding et al. [11] who proposed a method to predict salt rock damage based on the stress corresponding to the damage initiation point as the long-term strength. However, there are few studies on the relationship between critical stresses and long-term strength of hard brittle rocks, as well as creep characteristics under different critical stress intervals.

In this study, a series of laboratory tests, including uniaxial compression test, multistage loading creep test, and single-stage loading creep test, were carried out on sandstone specimens. The creep characteristics of specimens in

the interval of different critical stresses were investigated. The conclusions can provide reference for the analysis of time-dependent behavior of hard brittle rocks.

## 2. Specimen Preparation and Testing

The sandstones were obtained from Chongqing in China, whose natural dry density was approximately  $2.68 \times 10^3 \text{ kg/m}^3$ . Specimens made from sandstones had a columnar shape with a diameter of 50 mm and a height of 100 mm, which were in accordance with the standard recommended by the International Society for Rock Mechanics.

All the tests were performed on a HYZW-500L Rock Mechanics Testing System at the Key Laboratory of Geological Hazards on Three Gorges Reservoir Area, Ministry of Education, China. The loading rate of all tests was maintained at constant 0.2 kN/s. Firstly, uniaxial compression tests were carried out to obtain the critical stresses of the specimens. The axial stress  $\sigma_1$  was loaded on specimens progressively from 0 MPa until specimens were destroyed. Then, multistage loading creep tests were carried out to obtain the long-term strength.  $\sigma_1$  was loaded progressively from 0 MPa till the first stage of loading, and then it was increased to the next stage when the deformation was stable. Finally, the single-stage creep tests were performed, in which  $\sigma_1$  was set based on the results of the first two tests. After reaching the design level with the same loading procedure mentioned above,  $\sigma_1$  was kept constant until specimens were destroyed or the deformation was stable without increase (in this case, the loading time was at least 200 hours). The load, time, and displacements were recorded in all the tests.

## 3. Experimental Results

**3.1. Critical Stresses.** Based on the uniaxial compression test, the crack volumetric strain  $\varepsilon_v^c$ , the volumetric strain  $\varepsilon_v$ , and the elastic volumetric strain  $\varepsilon_v^e$  are calculated as follows [6]:

$$\begin{aligned} \varepsilon_v^c &= \varepsilon_v - \varepsilon_v^e \\ \varepsilon_v &= \varepsilon_1 + 2\varepsilon_3 \quad \}, \quad (1) \\ \varepsilon_v^e &= \frac{(1 - 2\mu)\sigma_1}{E} \end{aligned}$$

where  $\varepsilon_1$  is the axial strain,  $\varepsilon_3$  is the radial strain,  $\sigma_1$  is the stress level,  $E$  is the elastic modulus, and  $\mu$  is Poisson's ratio.

The  $\sigma_1$ - $\varepsilon_1$ - $\varepsilon_3$ ,  $\varepsilon_v$ - $\varepsilon_1$ , and  $\varepsilon_v^c$ - $\varepsilon_1$  curves of specimens are shown in Figure 1. According to the crack strain model method, the stress corresponding to the end of the concave section of the  $\sigma_1$ - $\varepsilon_1$  curve is point  $\sigma_{cc}$ , the stress corresponding to the beginning of the negative correlation between  $\varepsilon_v^c$  and  $\varepsilon_1$  in the  $\varepsilon_v^c$ - $\varepsilon_1$  curve is point  $\sigma_{ci}$ , and  $\sigma_{cd}$  is the value corresponding to the inflection point of the  $\varepsilon_v$ - $\varepsilon_1$  curve, after which the whole specimen starts to expand. Therefore, the critical stresses and deformation parameters of the sandstone specimen were  $\sigma_{cc} \approx 22.6 \text{ MPa}$ ,  $\sigma_{ci} \approx 50.3 \text{ MPa}$ ,  $\sigma_{cd} \approx 72.6 \text{ MPa}$ ,  $\sigma_c \approx 95.2 \text{ MPa}$ ,  $E \approx 11.2 \text{ GPa}$ , and  $\mu \approx 0.2$ .

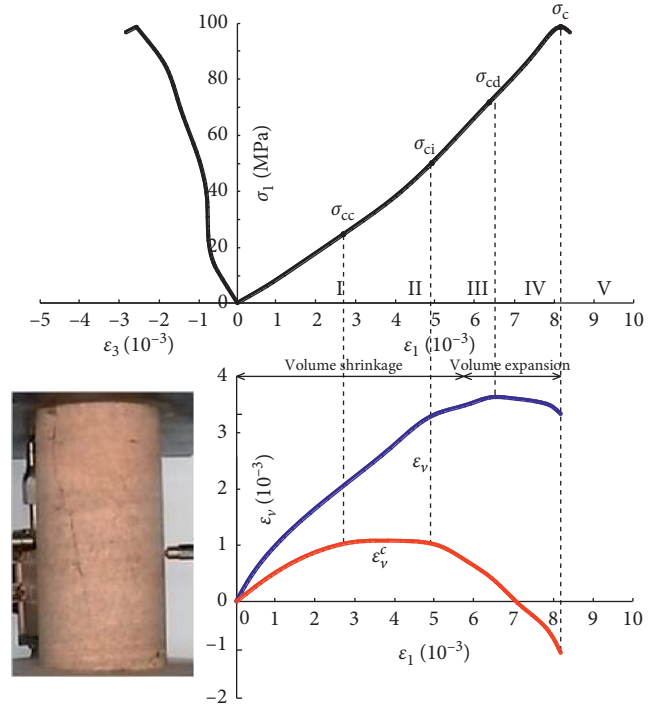


FIGURE 1: Uniaxial compression test curves and failure of the sandstone specimen.

**3.2. Long-Term Strength of the Isochronal Curve Method.** Based on the multistage loading creep tests, the time-dependent deformation curve under  $\sigma_1 = 50, 60, 70,$  and  $80 \text{ MPa}$  is shown in Figure 2. The deformations were stable after 24 h at  $\sigma_1 = 50, 60,$  and  $70 \text{ MPa}$ , while creep failure occurred after 17.4 h when  $\sigma_1 = 80 \text{ MPa}$ .

The isochronal curve composed of stress and strain values at loading time  $t$  of 2, 4, 8, 16, and 24 h is shown in Figure 3. The spacing between curves started to increase gradually from  $\sigma_1$  of 70 MPa, and the spacing with  $\sigma_1$  of 80 MPa between curves was significantly different from that of  $\sigma_1$  of 60 and 70 MPa. Therefore, the long-term strength of specimens was determined to be 70 MPa.

**3.3. Creep Rate of the Single-Stage Loading Creep Test.**

According to critical stresses of specimens and combined with results of the multistage loading creep test, the stress levels  $\sigma_1$  of the single-stage loading creep tests were designed to be 50, 60, 72, 74, 75, 80, and 85 MPa. From the test curves and specimen failures as shown in Figure 4, specimens did not fail under  $\sigma_1$  of 50, 60, and 72 MPa, while the accelerated creep stage and failure occurred under  $\sigma_1$  of 74, 75, 80, and 85 MPa, and the creep failure time gradually decreased to 139.5, 108.7, 42.2, and 17.5 h, respectively. The long-term strength obtained by the stress-strain isochronal curves was about 70 MPa, and the stress of creep failure in the single-stage loading creep tests was between 72 and 74 MPa, which was extremely close to the critical stress of dilation ( $\sigma_{cd} \approx 72.6 \text{ MPa}$ ) obtained in the uniaxial compression test. Therefore,  $\sigma_{cd}$  can be approximated as the long-term strength of specimens in this paper. It can be considered that

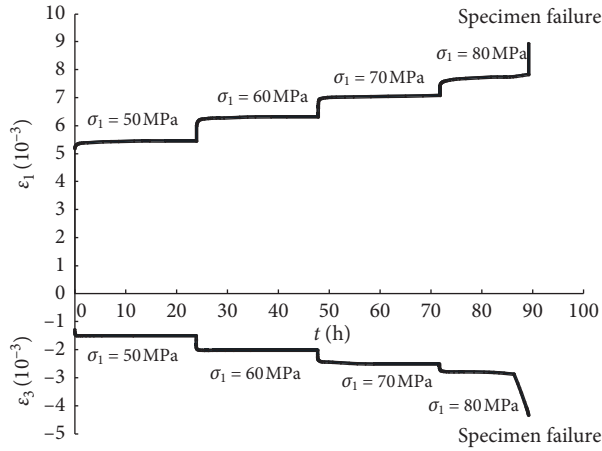


FIGURE 2: Creep deformation curves of the multistage creep test and failure of the specimen.

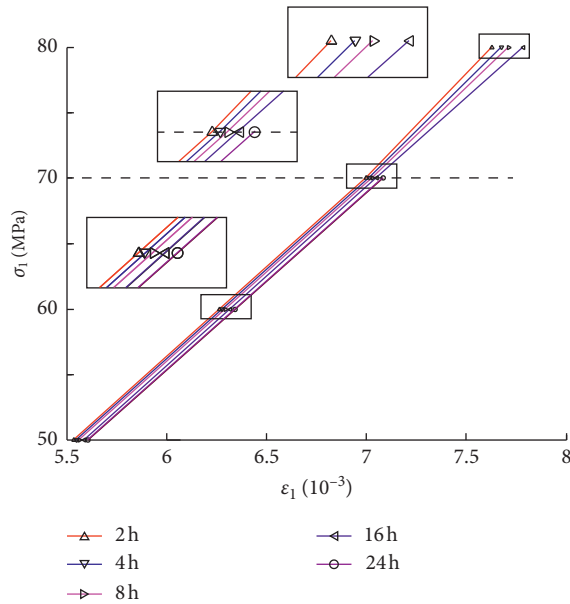


FIGURE 3: Stress-strain isochronal curves.

when  $\sigma_1$  is less than  $\sigma_{cd}$ , there will be no accelerated creep stage and no creep failure to specimens; when  $\sigma_1$  is greater than  $\sigma_{cd}$ , the accelerated creep stage and failure of specimens will occur.

As shown in Figure 4, the creep curves only showed characteristics of decay creeping, and the creep rate  $(d\varepsilon_1/dt)$  finally approaches 0 in the crack closure stage, elastic region, and stable crack growth stage ( $\sigma_1 < \sigma_{cd}$ ).

By analyzing the creep rate variation characteristics of four specimens at the accelerated creep stage shown in Figure 5, the steady-state creep stage of specimens was relatively short, which decreased with an increase of stress levels (the durations under  $\sigma_1$  of 74, 75, 80, and 85 MPa were 10.1, 6.0, 5.0, and 2.8 h, respectively). Yu et al. [12] showed that the time-dependent deformation exhibited is unstable in the secondary creep stage, and the results of the tests are similar. After the steady-state creep stage, there was a stage

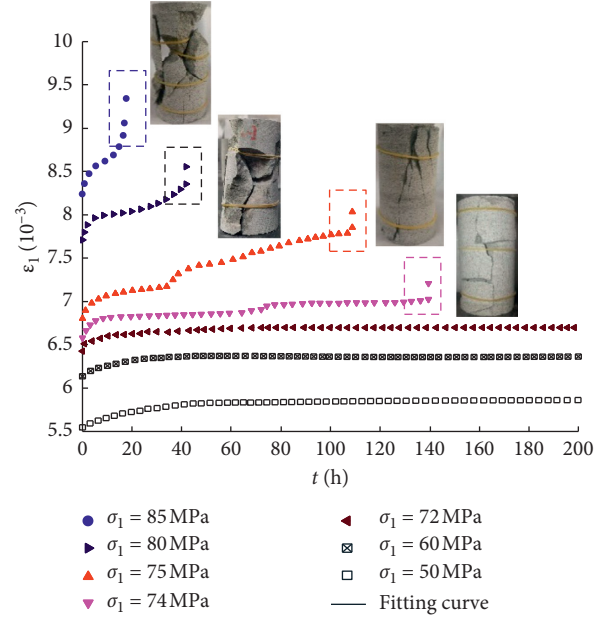


FIGURE 4: Creep deformation curves of the single-stage creep test and failure of the specimens.

of slowly increasing creep rate defined as stage III<sub>a</sub> (which is relatively evident in Figures 5(c) and 5(d)) in this paper. After stage III<sub>a</sub>, there was a stage in which the creep rate increases abruptly defined as stage III<sub>b</sub>; it was at the end of this stage that specimens failed. Due to the penetration and closure of some microfractures inside specimens under creep conditions, a steep increase and then a steep decrease of creep rate can be found in Figures 5(a) and 5(b). The failure modes of specimens were brittle failure, which is reflected in the creep curve as a sudden vertical ascent of the curve marked in Figure 4. The speed of the ascent was so fast that it presented a folded state rather than a smooth transition. Table 1 summarizes the creep rates and inclination angles of the marked area in Figure 4. There was a maximum creep rate  $(d\varepsilon_1/dt)_{max}$  at which specimens failed. And there was a positive correlation between  $(d\varepsilon_1/dt)_{max}$  and  $\sigma_1$ ; the larger  $\sigma_1$  was, the larger  $(d\varepsilon_1/dt)_{max}$  was.

## 4. Nonlinear Damage Creep Model

**4.1. Damage Variable.** Damage variable  $D$  is an important mechanical parameter for evaluating material properties and establishing the material damage model. When  $D = 0$ , there is no damage to the material; when  $D = 1$ , the material is fully damaged and loses its strength [13–17]. Combined with the test results, it was considered in this paper that when  $\sigma_1 < \sigma_{cd}$ , the specimens will not fail, and there is no damage to specimens; when  $\sigma_1 > \sigma_{cd}$ , the specimens will finally fail, and the damage exists in specimens. The damage has the following characteristics: (1) the damage is a time-dependent damage which increases gradually with time and finally reaches complete damage, namely,  $D = 1$ . (2) The damage is also affected by  $\sigma_1$ . The greater  $\sigma_1$  is, the shorter the time for specimens to reach the fully damaged state.

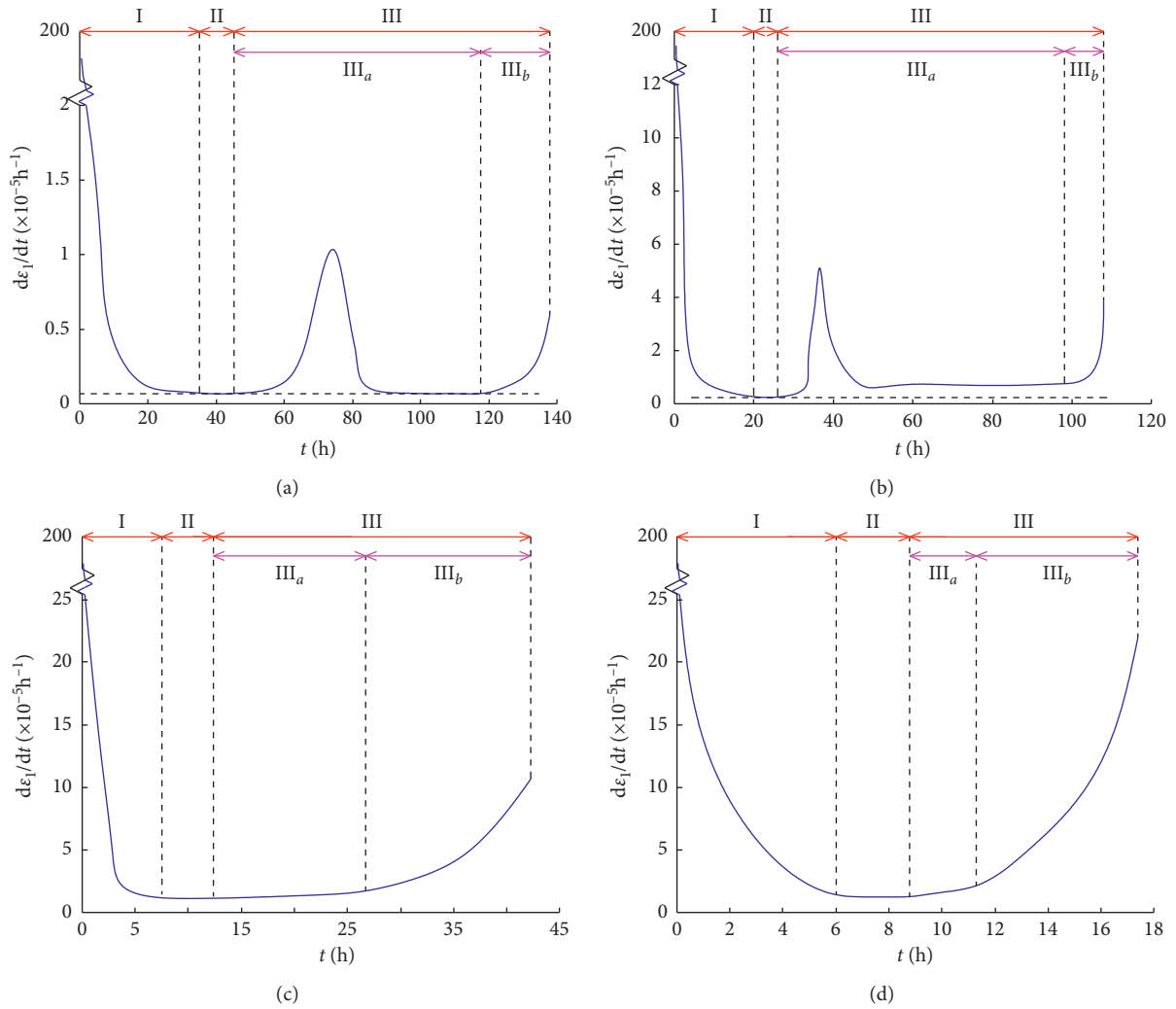
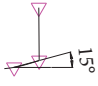
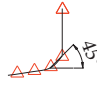
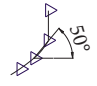
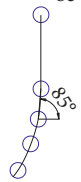


FIGURE 5: Creep rate curves of specimens under different stress levels: (a)  $\sigma_1 = 74$  MPa; (b)  $\sigma_1 = 75$  MPa; (c)  $\sigma_1 = 80$  MPa; (d)  $\sigma_1 = 85$  MPa.

TABLE 1: Creep rate and curve inclination before failure.

| $\sigma_1$ (MPa)                    | 74  | 75  | 80  | 85  |
|-------------------------------------|---|---|---|---|
| $(d\varepsilon_1/dt)_{\max}/h^{-1}$ | $0.63 \times 10^{-5}$   | $3.67 \times 10^{-5}$   | $10.00 \times 10^{-5}$  | $22.00 \times 10^{-5}$  |
| Inclination angles ( $^\circ$ )     | 15  | 45  | 50  | 85  |
| Creep curve before failure          |  |  |  |  |

In terms of the strength of specimens, creep failure occurred in specimens under  $\sigma_1$  of 74, 75, 80, and 85 MPa, which was reduced by 23%, 21%, 16%, and 10% compared with  $\sigma_c$ .

In terms of the deformation of specimens, the viscosity coefficient  $\eta$  at each time in the creep process can be expressed as

$$\frac{d\varepsilon_1}{dt} = \frac{\sigma_1}{\eta}. \quad (2)$$

When  $\sigma_1$  is constant, the creep rate  $d\varepsilon_1/dt$  is inversely proportional to  $\eta$ . As shown in Figure 5, the creep rate of the specimen was constant in stage II and began to increase as it entered stage III, which indicates that  $\eta$  began to decay with

increasing creep time. Therefore, it can be assumed that no time dependence was produced before stage III, while it started to appear after stage III. When  $\sigma_1$  was 74, 75, 80, and 85 MPa,  $\eta$  of creep failure was lost about 92%, 90%, 99%, and 95%, respectively.

It was obvious that the damage of the specimen in strength was very different from that in deformation, and the same damage variable cannot be used to describe both. Therefore, two types of damage variables, named strength damage variable and deformation damage variable, were proposed from the analysis above.

The strength damage variable  $D_1(\sigma, t)$  can be calculated as

$$D_1(\sigma, t) = \frac{\sigma_c - \sigma_f(t)}{\sigma_c - \sigma_1}, \quad (3)$$

where  $\sigma_1$  is the long-term load applied on specimens and  $\sigma_f(t)$  is the stress corresponding to the creep failure time  $t$ .

When  $\sigma_f(t) = \sigma_c$ , specimens are instantaneously damaged, namely,  $t = 0$ . When  $\sigma_f(t) = \sigma_{cd}$ , the specimen will be permanently undamaged, namely,  $t = \infty$ . Combined with the stress and time corresponding to the creep failure of specimens in the single-stage loading creep test, the fitting curve is presented in Figure 6.

It can be seen from Figure 6 that the larger  $\sigma_1$  was, the shorter the time required for the creep failure of specimen  $t_f$  was. This relationship can be described as

$$\sigma_f(t_f) = \sigma_{cd} + (\sigma_c - \sigma_{cd})\exp(-\alpha t_f), \quad (4)$$

where  $\alpha$  is the correlation coefficient of damage degree, which can be fitted according to the test data. For specimens in this paper,  $\alpha = -0.025$ . By combining equations (3) and (4), the expression of strength time-dependent damage variable  $D_1(\sigma, t)$  of specimens can be described as

$$D_1(\sigma, t) = \frac{(\sigma_c - \sigma_{cd})(1 - \exp(-\alpha t))}{\sigma_c - \sigma_1}. \quad (5)$$

The deformation damage variable  $D_2(\sigma, t)$  of specimens proposed in this paper is

$$D_2(\sigma, t) = \begin{cases} 0, & t \leq t_w, \\ 1 - [\eta(\sigma, t)/\eta_0], & t > t_w, \end{cases} \quad (6)$$

where  $\eta(\sigma, t)$  is the viscosity coefficient function with creep time  $t$ ,  $\eta_0$  is the viscosity coefficient at the steady-state creep stage, and  $t_w$  is the time required to reach stage III<sub>a</sub>.

Creep failure of specimens occurred when  $D_1(\sigma, t) = 1$ , while  $D_2(\sigma, t)$  is not strictly equal to 1, and  $\eta(\sigma, t)$  corresponded to the maximum creep rate  $(d\varepsilon_1/dt)_{\max}$  as described in Table 1.

Figure 7 shows the relationship between  $t_w$  and  $\sigma_1$  and the variation of  $\eta(\sigma, t)$  with time. The larger  $\sigma_1$  is, the shorter the time experienced before entering the steady-state creep stage is and the small  $\eta$  in the steady-state creep stage is. Moreover,  $\eta(\sigma, t)$  decreases gradually with time after stage II; this relationship can also be described as

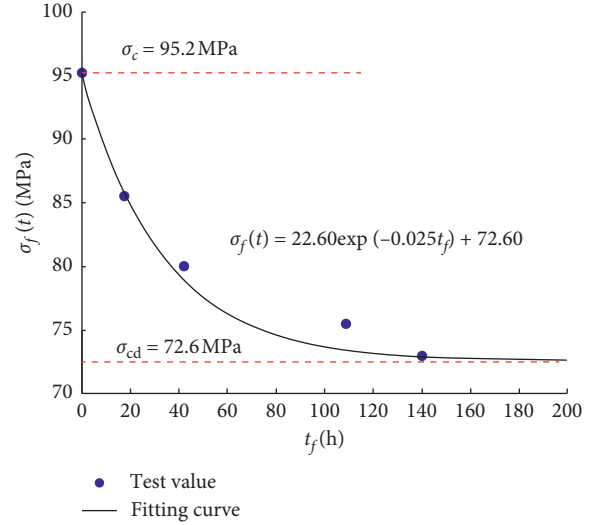


FIGURE 6: Relationship between load and time in the creep failure of specimens.

$$\eta(\sigma, t) = \begin{cases} \eta_0, & t \leq t_w, \\ \eta_0 \exp(-\beta t), & t > t_w, \end{cases} \quad (7)$$

where  $\beta$  is the correlation coefficient of damage degree, which is related to  $\sigma_1$ . As  $\sigma_1$  increases,  $\beta$  increases gradually. The fitting curve combined with  $\eta_0$ ,  $\beta$ , and  $\sigma_1$  is shown in Figure 8.

It can be observed that, with the increase of  $\sigma_1$ ,  $\eta_0$ , and  $\beta$ , different variation laws were shown:  $\eta_0$  decreased with  $\sigma_1$ , while  $\beta$  increased with  $\sigma_1$ . By combining equations (6) and (7), the expression of deformation time-dependent damage variable  $D_1(\sigma, t)$  can be described as

$$D_2(\sigma, t) = \begin{cases} 0, & t \leq t_w, \\ 1 - \exp(-\beta t), & t > t_w. \end{cases} \quad (8)$$

**4.2. A New Damage Creep Model with Different Critical Stress Intervals.** Based on the creep characteristics and two damage variables of specimens, a new 5-element nonlinear damage creep model was established, in which  $\sigma_{cd}$  is the stress threshold that controls the damaged viscous element, as shown in Figure 9.

According to equation (7), the nonlinear expression of the constitutive equation of the damaged viscous element can be obtained as

$$\frac{d(\varepsilon_1)}{dt} = \frac{\sigma_1}{\eta_0} \exp(\beta t). \quad (9)$$

Taking  $\varepsilon_1 = 0$  when  $t = 0$ , the creep equation of the damaged viscous element can be written as

$$\varepsilon_1 = \frac{\sigma_1}{\eta_0 \beta} [\exp(\beta t) - 1]. \quad (10)$$

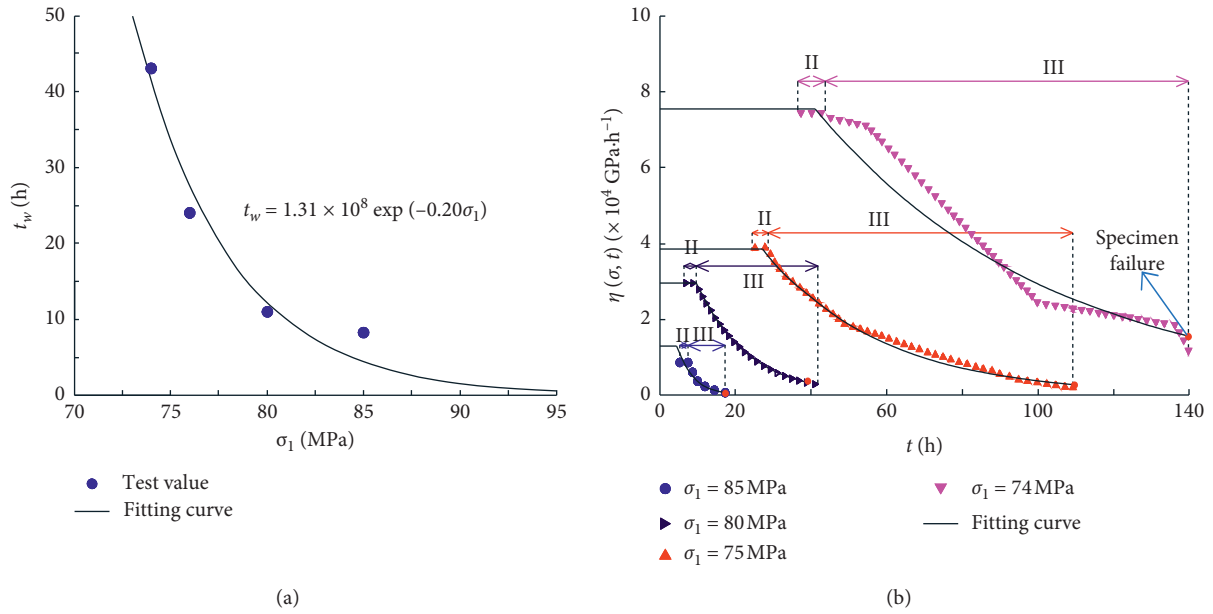


FIGURE 7: Relationship between  $t_w$  and  $\sigma_1$  and  $\eta(\sigma, t)$  and  $t$ : (a)  $t_w$ - $\sigma_1$ ; (b)  $\eta(\sigma, t)$ - $t$ .

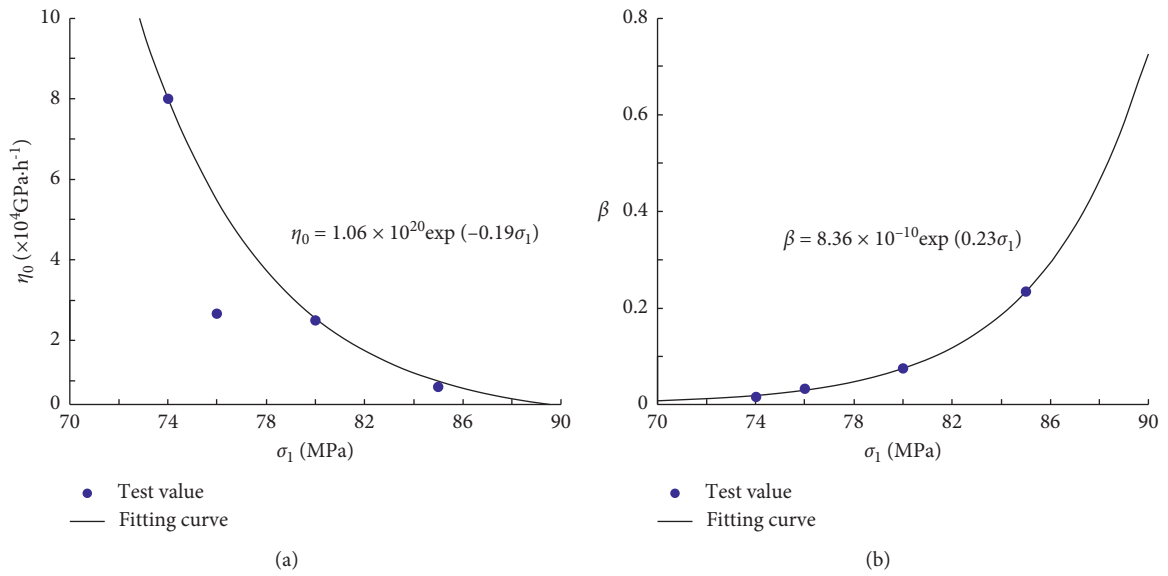


FIGURE 8: The relation graph of viscosity coefficient  $\eta_0$ - $\sigma_1$  and  $\beta$ - $\sigma_1$  in stage II of the specimen: (a)  $\eta_0$ - $\sigma_1$ ; (b)  $\beta$ - $\sigma_1$ .

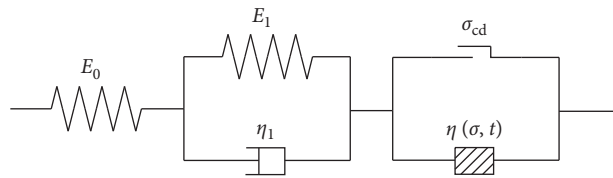


FIGURE 9: Damage creep models with different critical stress intervals.

TABLE 2: The parameters of the damage creep model for specimens.

| $\sigma_1$ (MPa) | $E_0$ (GPa) | $E_1$ (GPa) | $\eta_1 \cdot (\text{GPa} \cdot \text{h})$ | $\eta_0 \cdot (\text{GPa} \cdot \text{h})$ | $\beta$ |
|------------------|-------------|-------------|--|--|---------|
| 50               | 9.3         | 160         | 500  | —  | —       |
| 60               | 9.93        | 170         | 600  | —  | —       |
| 72               | 11.35       | 195         | 600  | —  | —       |
| 74               | 11.03       | 300         | 900  | 80000                                      | 0.01884 |
| 75               | 11.11       | 300         | 900  | 55000                                      | 0.02978 |
| 80               | 10.45       | 300         | 600  | 25000                                      | 0.07400 |
| 85               | 10.39       | 300         | 600  | 9800                                       | 0.23350 |

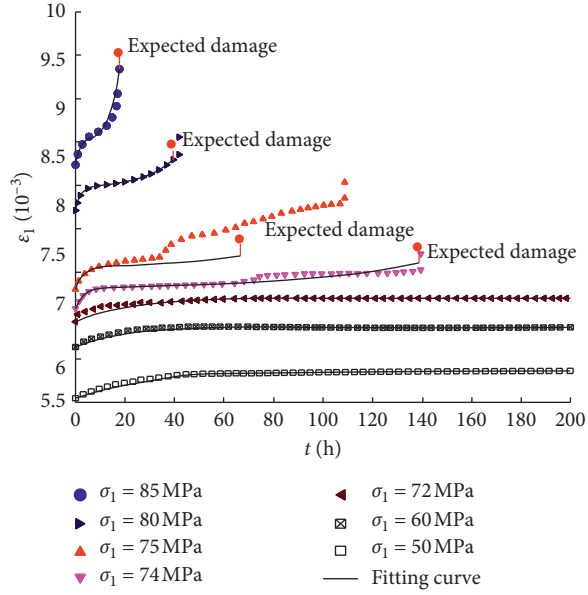


FIGURE 10: The scatter plot of one-step loading creep test and its fitting curve.

Substituting equation (7) into the generalized Kelvin model, the equation of the nonlinear damage creep model can be determined as follows.

- (1) When in the crack closure stage, elastic region, and stable crack growth stage ( $\sigma_1 < \sigma_{cd}$ ), the damage creep model is a generalized Kelvin model; then, the equation is

$$\varepsilon(\sigma, t) = \frac{\sigma_1}{E_0} + \frac{\sigma_1}{E_1} \left( 1 - \exp\left(-\frac{E_1}{\eta_0} t\right) \right). \quad (11)$$

- (2) When in the unstable crack growth stage ( $\sigma_1 > \sigma_{cd}$ ), the damage creep model is made up of generalized Kelvin model in series with a damaged viscous element, and the equation is

$$\varepsilon(\sigma, t) = \begin{cases} \frac{\sigma_1}{E_0} + \frac{\sigma_1}{E_1} \left( 1 - \exp\left(-\frac{E_1}{\eta_1} t\right) \right) + \frac{\sigma_1}{\eta_0} t, & t \leq t_w, \\ \frac{\sigma_1}{E_0} + \frac{\sigma_1}{E_1} \left( 1 - \exp\left(-\frac{E_1}{\eta_1} t\right) \right) + \frac{\sigma_1}{\eta_0 \beta} [\exp(\beta t) - 1], & t > t_w. \end{cases} \quad (12)$$

Table 2 shows the fitting values of parameters, and Figure 10 shows the comparison of creep fitting curves and test curves. It can be observed that the damage creep model can better describe all three stages of the creep process and can accurately predict the creep failure time of specimens. Due to the influence of specimen discreteness, the fitting effect under 75 MPa is poor.

## 5. Conclusions

- (1) Creep tests were carried out, and the creep deformation curves of sandstone in the interval of different critical stresses were acquired. The test results showed that the long-term strength is very close to the critical stress of dilation.
- (2) Two new damage variables to describe the time-dependent damage of hard brittle rocks were proposed. The creep failure time of specimens was controlled by the strength damage variable, and the deformation of specimens was controlled by the deformation damage variable.
- (3) The nonlinear damage creep models with different critical stress intervals can well match the test data and predict the creep failure time and deformation of specimens in the creep process. They can also describe the phenomenon that the creep failure mode of hard brittle rocks was brittle failure.
- (4) Further research will be carried out in the numerical calculation of the damage model established in this paper, so as to realize the application in practical engineering.

## Data Availability

The datasets generated and/or analysed during the current study are available from the first author upon reasonable request.

## Conflicts of Interest

The authors declare that they have no conflicts of interest.

## Acknowledgments

This work was supported by the <https://dx.doi.org/10.13039/501100001809> National Natural Science Foundation of China (nos. 51909136, U1965109, and 51809151).

## References

- [1] E. Eberhardt, D. Stead, B. Stimpson, and R. S. Read, "Identifying crack initiation and propagation thresholds in brittle rock," *Canadian Geotechnical Journal*, vol. 35, no. 2, pp. 222–233, 1998.
- [2] Y.-H. Gao, X.-T. Feng, X.-W. Zhang, G.-L. Feng, Q. Jiang, and S.-L. Qiu, "Characteristic stress levels and brittle fracturing of hard rocks subjected to true triaxial compression with low minimum principal stress," *Rock Mechanics and Rock Engineering*, vol. 51, no. 12, pp. 3681–3697, 2018.
- [3] C. D. Martin and N. A. Chandler, "The progressive fracture of Lac du Bonnet granite," in *Proceedings of International Journal of Rock Mechanics and Mining Science & Geomechanics Abstracts*, Pergamon, Turkey, 1994 December.
- [4] N. A. Chandler, "Quantifying long-term strength and rock damage properties from plots of shear strain versus volume strain," *International Journal of Rock Mechanics and Mining Sciences*, vol. 59, pp. 105–110, 2013.
- [5] B. Damjanac and C. Fairhurst, "Evidence for a long-term strength threshold in crystalline rock," *Rock Mechanics and Rock Engineering*, vol. 43, no. 5, pp. 513–531, 2010.
- [6] C. D. Martin, *The strength of massive Lac du Bonnet granite around underground openings*, UMI Dissertation Services, Michigan, US, 1993.
- [7] M. E. Kassner, *Fundamentals of Creep in Metals and Alloys*, Butterworth-Heinemann, Oxford, UK, 2015.
- [8] H. Özsen, İ. Özkan, and C. Sensögüt, "Measurement and mathematical modelling of the creep behaviour of Tuzköy rock salt," *International Journal of Rock Mechanics and Mining Sciences*, vol. 66, pp. 128–135, 2014.
- [9] R. Wang, Y. Jiang, C. Yang, F. Huang, and Y. Wang, "A nonlinear creep damage model of layered rock under unloading condition," *Mathematical Problems in Engineering*, vol. 2018, pp. 1–8, 2018.
- [10] X. Liu, *Rock Rheology Introduction*, Geological Publishing, Beijing, China, 1994.
- [11] G. Ding, J. Liu, L. Wang, Z. Wu, and Z. Zhou, "Discussion on determination method of long-term strength of rock salt," *Energies*, vol. 13, no. 10, p. 2460, 2020.
- [12] J. Yu, G. Liu, Y. Cai, J. Zhou, S. Liu, and B. Tu, "Time-dependent deformation mechanism for swelling soft-rock tunnels in coal mines and its mathematical deduction," *International Journal of Geomechanics*, vol. 20, no. 3, Article ID 04019186, 2020.
- [13] D. Gu, H. Liu, X. Gao, D. Huang, and W. Zhang, "Influence of cyclic wetting–drying on the shear strength of limestone with a soft interlayer," *Rock Mechanics and Rock Engineering*, pp. 1–10, 2021.
- [14] Q. Jiang, J. Cui, and J. Chen, "Time-dependent damage investigation of rock mass in an in situ experimental tunnel," *Materials*, vol. 5, no. 8, pp. 1389–1403, 2012.
- [15] Q.-X. Meng, W.-Y. Xu, H.-L. Wang, X.-Y. Zhuang, W.-C. Xie, and T. Rabczuk, "DigiSim - an open source software package for heterogeneous material modeling based on digital image processing," *Advances in Engineering Software*, vol. 148, Article ID 102836, 2020.
- [16] Y. Wang, W. K. Feng, R. L. Hu, and C. H. Li, "Fracture evolution and energy characteristics during marble failure under triaxial fatigue cyclic and confining pressure unloading (FC-CPU) conditions," *Rock Mechanics and Rock Engineering*, vol. 54, no. 2, pp. 799–818, 2021.
- [17] H. Zhao, C. Shi, M. Zhao, and X. Li, "Statistical damage constitutive model for rocks considering residual strength," *International Journal of Geomechanics*, vol. 17, no. 1, Article ID 04016033, 2017.